SURFACE AND INTERFACE ANALYSIS, VOL. 25, 390–396 (1997)

Charging Phenomena and Charge Compensation in AES on Metal Oxides and Silica

Hansheng Guo, W. Maus-Friedrichs* and V. Kempter
Physikalisches Institut der Technischen Universität Clausthal, Leibnizstr. 4, D-38678 Clausthal-Zellerfeld, Germany

Charging processes on the bulk oxides Al_2O_3, ZrO_2 and SiO_2 occurring during Auger Electron Spectroscopy (AES) are studied. All samples experience a negative charge-up under the following parameters: electron beam energy >1 keV, current density $>10^{-2}$ A cm^{-2} and different angles of incidence. The samples show strong history effects as a function of previous irradiation damage. For charge compensation, Environmental Auger Electron Spectroscopy with O_2 gas is applied; several traditional methods were applied for comparison. Charging of SiO_2 and ZrO_2 could be reduced considerably in an O_2 environmental pressure of $<5 \times 10^{-8}$ Torr. Charging of Al_2O_3 could be compensated completely in this oxygen environment. It is shown that for the compensation of the electron beam effects, including electron-stimulated desorption and carbon contamination of the surface, an O_2 atmosphere of 5×10^{-8} Torr is more efficient than using an auxiliary electron gun or low-energy positive ions. It is also more efficient than an Ar environment of 1×10^{-4} Torr. © **1997 by John Wiley & Sons, Ltd.**

Surf. Interface Anal. **25**, 390–396 (1997)
No. of Figures: 7 No. of Tables: 2 No. of Refs: 16

KEYWORDS: Environmental AES; Electron-Stimulated Desorption; insulating surfaces; aluminium oxide; silicon oxide

INTRODUCTION

Auger Electron Spectroscopy (AES) is a powerful surface analysis tool for the determination of the surface chemical composition and even the electronic structure. The electron beam can be focused down to submicron diameters and can be scanned to perform lateral resolved analysis, but charging phenomena occur for a wide variety of insulating materials in AES. The charging processes are complicated and poorly understood; even among the oxides Al_2O_3, SiO_2 and ZrO_2, the charging behaviour is different and sample history-dependent. A systematic study of the charging phenomena is essential for a better understanding of the microscopic mechanisms of charging and for exploring efficient methods for charge reduction.

In order to avoid charging effects, several approaches have been made.[1,2] The harmful effects of some methods are summarized in Refs 2 and 3. For AES on insulators, the disadvantages in applying an auxiliary electron gun, a positive ion flux, deposition of a conducting layer on the analysed surface and the growth of an insulating film on a conducting substrate are summarized here briefly.

For the reduction of negative charges, an auxiliary electron gun offering an electron beam of several hundred electron-Volts is often used. However, it enhances Electron Stimulated Desorption (ESD) on many compounds; the additional elastic peak and the enhancement of the Auger intensities make the spectrum unusable at energies less than that of the auxiliary beam.[2] Charge reduction utilizing positive ions, e.g. an Ar^+ beam (500 eV), is accompanied by sputtering, which is obviously not advisable for the analysis of irradiation-sensitive materials and layers or film samples. A conducting layer weakens the Auger signals of the underlaying insulating sample; the additional Auger peaks from the conducting layer and the possible interaction in the interface can disturb the spectrum significantly. The backscattering coefficient of the electrons that contribute to the Auger intensities is dependent on the substrate material.[4] On the other hand, the composition and structure of an insulating film grown on the conducting substrate is often different from that of the bulk insulator.

For convenience, compromises are made in the set-up of the primary parameters, thus reducing lateral resolution and the signal-to-noise ratio in AES. For the efficiency of other methods of charge compensation, we found only scarce experimental information. Ichimura *et al.*[2] have used an auxiliary gun, an Ar^+ beam (500 eV) and prepared thin Ag layers on the surface to reduce the charging of insulating substances; it has been shown that all these methods could reduce the charging of Si_3N_4. The charging of single crystals and polycrystalline samples of Al_2O_3 could be avoided by applying an auxiliary gun and an Ar^+ beam (500 eV). However, perturbation of the spectrum by the Ag layer and the auxiliary gun made quantitative Auger analysis difficult. It was not mentioned whether these methods are applicable for long-term irradiation, because on some insulating materials, such as crystalline Al_2O_3, charging normally appears after many hours of irradiation.[5] Ohlendorf *et al.*[6] have applied Environmental Electron Spectroscopy to AES of bulk ceramics: the specimen under study is held in a controlled gaseous

* Correspondence to: W. Maus-Friedrichs, Physikalisches Institut der Technischen Universität Clausthal, Leibnizstr. 4, D-38678 Clausthal-Zellerfeld, Germany

Contract grant sponsor: Deutsche Forschungsgemeinschaft; grant no.: SFB 180.

CCC 0142–2421/97/060390–07 $17.50

Received 27 September 1996
Accepted 23 January 1997

environment. At relatively high pressures a sufficiently large number of gas molecules are ionized by the primary and secondary electrons. This leads to a reduction of the negative charge and was explained as caused by an Auger Neutralization (AN) process between the created ion and the charged defects at the surface. It was found that Al_2O_3 in an Ar atmosphere of 1×10^{-4}–5×10^{-4} Torr is charge-free for many hours.[6] However, this Ar pressure is too high to keep the analysed surface free from other contamination. In addition, we find that the Ar environment does not prevent the charging up of other oxides such as ZrO_2.

After a systematic observation and analysis of the charging phenomena we decided to introduce environmental electron spectroscopy with O_2 for AES on oxides. The O_2 atmosphere is efficient in charge compensation over a period of days on the samples studied; ESD of oxygen and contamination of the surface from residual gas was also reduced. It will be shown that a satisfactory compensation of all the irradiation effects on Al_2O_3 is achieved in 5×10^{-8} Torr O_2. The advantages will be demonstrated by comparison with other methods. An attempt will be made to clarify the underlying mechanisms for the charge compensation.

EXPERIMENTAL

A Scanning Auger Microprobe (PHI SAM 545) was used for AES of insulating materials; a partial description of the apparatus can be found in Ref. 6. The central electron gun in the cylindrical mirror analyser (CMA) provided a stable electron beam with a primary energy up to 8 keV. For a fixed electron beam focus with a constant emission, the beam diameter decreases with increasing primary energy. The beam diameter and the electron current are determined by a Faraday cup with a 1.2 mm opening. The parameters used in this work are listed in Table 1.

The following devices were added for reduction of negative charge-up:

(1) An auxiliary electron gun (LEG32, VG Instruments) was mounted at a fixed angle of 60° to the specimen surface normal. This electron beam with a fixed energy of 400 eV has a beam diameter on the specimen surface of ~2.5 mm.
(2) An ion gun (Specs 10 867) was mounted at an incident angle of 60°. In order to reduce the charging of the specimen in AES, this ion was operated with Ar gas; for this purpose, the ion energy was set to 500 eV with a current density of $\sim 5 \times 10^{-6}$ A cm^{-2}. The pressure in the analysis chamber was kept in the low 5×10^{-10} Torr range during the use of the electron sources, while the analysis chamber was filled with 2×10^{-7} Torr Ar when the ion gun was used.

Specimen heating is also available. A filament is installed on the manipulator in front of the CMA. Utilizing thermoemission, a temperature of ~400 °C on the sample supports can be achieved; applying a negative bias of 600 V to the filament, ~650 °C on the sample supports can be achieved. The temperature is measured by a W–Re3%–W–Re25% thermocouple. Because of the poor thermoconductivity of the insulating materials the measured temperature on the sample surface could be underestimated seriously. Throughout this paper the temperature of the sample supports is given.

Helium and O_2 are used for Environmental AES.[6] Argon gas fills the apparatus via the ion gun; He and O_2 are offered via an additional dosage valve. In the experiment the Ar and He pressures are kept below 1×10^{-4} Torr and O_2 below 5×10^{-8} Torr. In environmental AES the sputter-ion pump is shut down; instead, a turbomolecular pump maintains the desired gas pressure.

The samples studied are single crystalline Al_2O_3, ZrO_2 stabilized with 9 mol.% Y_2O_3 (YS–ZrO_2) and amorphous SiO_2 (a-SiO_2). The samples have a thickness of ~1 mm. Before inserting the sample into the analysis chamber, they were cleaned in acetone in an ultrasonic bath and then rinsed with distilled water. All surfaces were then cleaned by sputtering with Ar^+ (2 keV, $\sim 6 \times 10^{-5}$ A cm^{-2}) until any carbon contamination in the AES spectra has disappeared. AES on a-SiO_2 is performed at a primary incident angle of 30° and 60° to the specimen surface normal; AES on Al_2O_3 and YS–ZrO_2 is performed using 30° and normal primary incidence.

Table 1. Applied primary parameters[a]

Primary energy E_P (keV)	Primary current I_P (μA)	Beam diameter a_s (μm)	Primary current density J_P ($\times 10^{-2}$ A cm^{-2}) $\alpha = 0°$	$\alpha = 30°$	$\alpha = 60°$
1	1.8	230	0.4	0.37	0.22
2	2	200	0.6	0.55	0.32
3	2.5	160	1.2	1.08	0.62
5	2.5	100	3.2	2.76	0.59
8	2.5	20	79.6	68.95	39.80

[a] α denotes the incident angle with respect to the surface normal.

RESULTS

Charging phenomena

In the present experiment all samples charge negatively when applying primary electron energies $\geqslant 1$ keV and incident angles $\leqslant 30°$ measured with respect to the specimen surface normal. However, the charging phenomena differ in the charge-up behaviour and in the charge potential at saturation. As reported by Le Gressus *et al.*[5] for a freshly cleaned Al_2O_3, a significant charge appears only after an irradiation period of more than 10 h; similarly, when first exposed to the electron beam, a strong charging of YS–ZrO_2 is observed after several hours. By contrast, electron bombardment of SiO_2 leads to an immediate strong charge-up, and the time interval to reach the saturation potential is much shorter.

In Fig. 1 the differentiated spectrum displays a splitting of the O $KL_{2,3}L_{2,3}$ peak in the initial stage of charging of the Al_2O_3 sample bombarded with 2 keV electrons at normal incidence. The energy positions of the split peaks are traced by the dotted lines, and the target current is indicated for each spectrum. The elec-

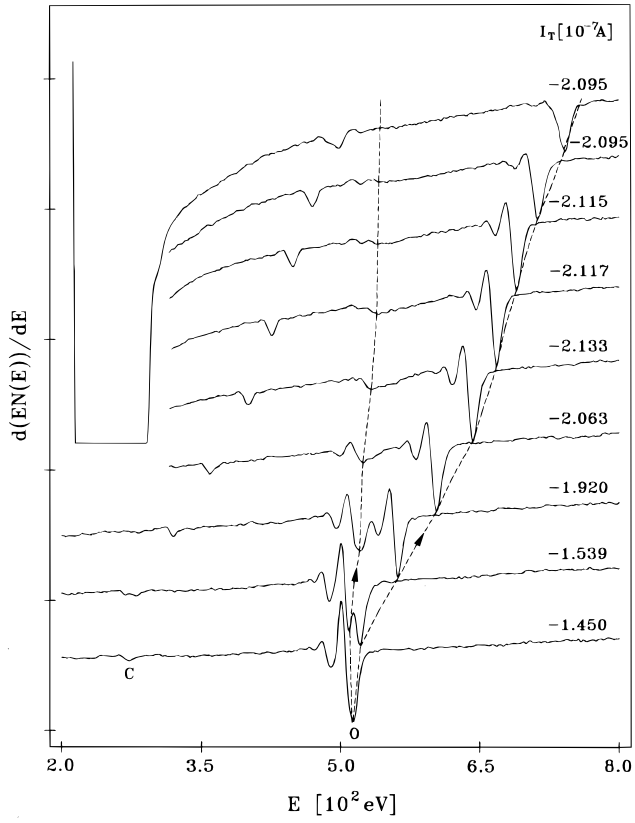

Figure 1. The splitting of the O $KL_{2,3}L_{2,3}$ peak at the start of charging on Al_2O_3. The energy positions of the split peaks are tracked by the dotted line. For each spectrum the target current is indicated. ($E_P = 2$ keV, $\alpha = 0°$.)

tron beam effects on the samples could be preserved under UHV conditions (5×10^{-10} Torr base pressure) for days: on the three samples only small discharging could be observed in the first hours after irradiation. This history effect could not be eliminated completely, even after the irradiated zone has been discharged.

Figure 2 shows the charging potential (U_C) as a function of irradiation time for the Al_2O_3 sample for the first and second exposures to 8 keV electrons at 30° incidence; before bombarding for the second time, the irradiated zone was discharged completely in 1×10^{-4} Torr Ar.

Methods for charge reduction

Traditional methods. With an auxiliary low-energy electron beam no charge compensation on Al_2O_3 can be achieved for primary energies >4 keV and incidence angles $<30°$. Figure 3 shows the time dependence of the charge potential with and without the auxiliary electron beam; the charge reduction is effective only in the beginning of the exposure.

Another possibility for enhancing the secondary electron yield can be achieved by a positive bias on the irradiated surface. For this purpose the top point of the thermocouple (diameter 0.15 mm) was pressed on the surface close to the irradiated zone, and a positive potential up to 150 V was applied. With increasing bias voltage a rise of the secondary emission was observed, and simultaneously a reduction of the charge potential on the Al_2O_3 sample, although complete compensation could not be achieved.

Applying an Ar^+ beam (500 eV), charge reduction on Al_2O_3 is more efficient than with the auxiliary electron beam; however, the simultaneous alignment of the ion beam to its maximal density and to the primary electron beam spot on the sample surface is a tedious procedure. In this experiment a charge compensation for primary energies up to 5 keV has been achieved.

In Environmental AES using Ar on He (1×10^{-4} Torr), slow ions (Ar^+, He^+) lead to charge reduction on Al_2O_3; under electron bombardment with primary energies >3 keV and incidence $\leqslant 30°$, the Al_2O_3 sample is charge free. These findings agree with those reported by Ohlendorf *et al.*[6] At primary energies $\leqslant 3$ keV, which introduce stronger damage at the surface than higher primary energies, an oxygen deficiency and carbon contamination could not be avoided and some charging appeared occasionally.

Heating of the Al_2O_3 sample to 600 °C does not prevent the charging phenomenon for primary energies >5 keV. Note that as specimen heating enhances ESD of oxygen, this method is not useful for AES analysis. The charge potentials as a function of specimen heating

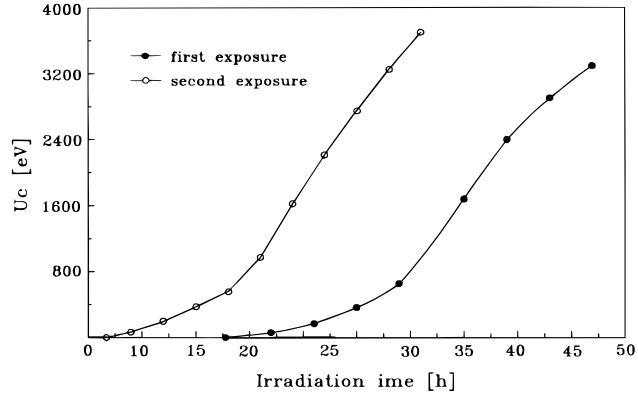

Figure 2. The charging processes under the first and second electron beam irradiation period on the same spot of the Al_2O_3 surface. Before the second bombardment the irradiated zone has been discharged completely in 1×10^{-4} Torr Ar. ($E_P = 8$ keV, $\alpha = 30°$.)

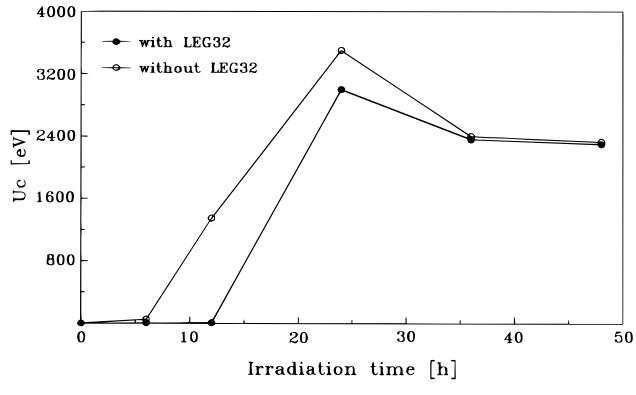

Figure 3. The charge potentials with and without 'charge compensation' using the auxiliary electron gun (400 eV) in AES on Al_2O_3.

Table 2. Charge potentials (eV) on Al_2O_3 under 5 and 8 keV electron irradiation for 30° incident angle and different temperatures

	Temperature (°C)					
	315	445	460	495	550	600
$E_P = 5$ keV	1030	1090	1120	730	120	10
$E_P = 8$ keV	700	1550	2300	1730	1100	330

are given in Table 2 for the Al_2O_3 sample for primary energies of 5 and 8 keV.

Charge reduction in oxygen. An O_2 atmosphere turned out to be a promising environment for AES investigations on oxides: pressure as low as 5×10^{-9} Torr lead to a reduction in charging. In 2×10^{-8} Torr O_2 the charging potential on Al_2O_3 under bombardment with 8 keV electrons at 30° incidence for 2 days does not exceed 35 eV; by applying 5×10^{-8} Torr O_2 the charging problem could be avoided completely for all primary energies and primary incidence angles. In addition, neither oxygen deficiency nor carbon contamination appeared at primary energies $\geqslant 3$ keV and primary incidences $\leqslant 30°$. For primary energies < 3 keV and incidence angles $> 30°$ carbon contamination cannot be avoided completely. Figure 4 shows the spectra of Al_2O_3 obtained under irradiation with 8 keV electrons at normal incidence; the irradiation time is indicated. In

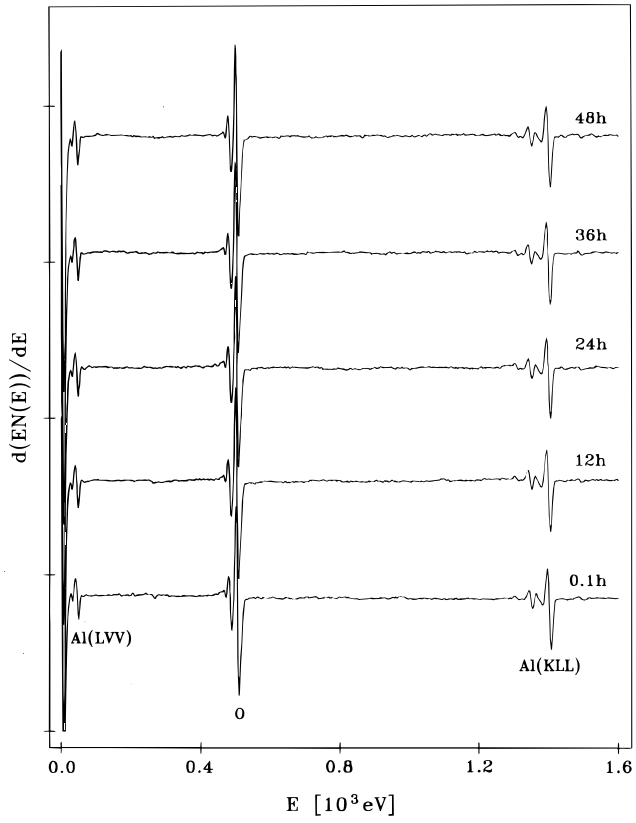

Figure 4. The charge-compensated spectra of Al_2O_3 in 5×10^{-8} Torr O_2. Irradiation time is indicated in each spectrum. ($E_P = 8$ keV, $\alpha = 0°$.)

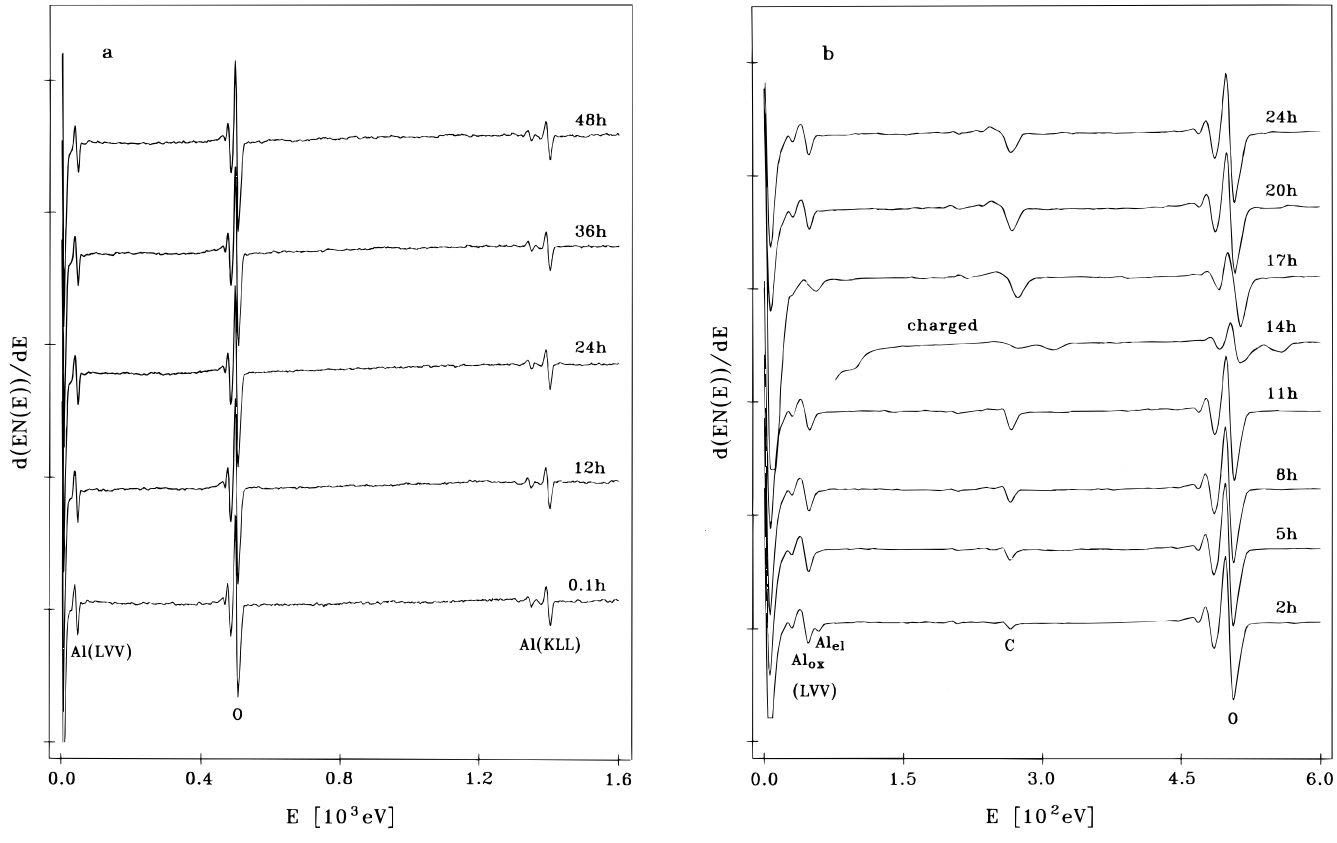

Figure 5. The spectra of Al_2O_3 in environmental AES in: (a) 5×10^{-8} Torr O_2; (b) 1×10^{-4} Torr Ar. Irradiation time is indicated in each spectrum. ($E_P = 3$ keV, $\alpha = 30°$.)

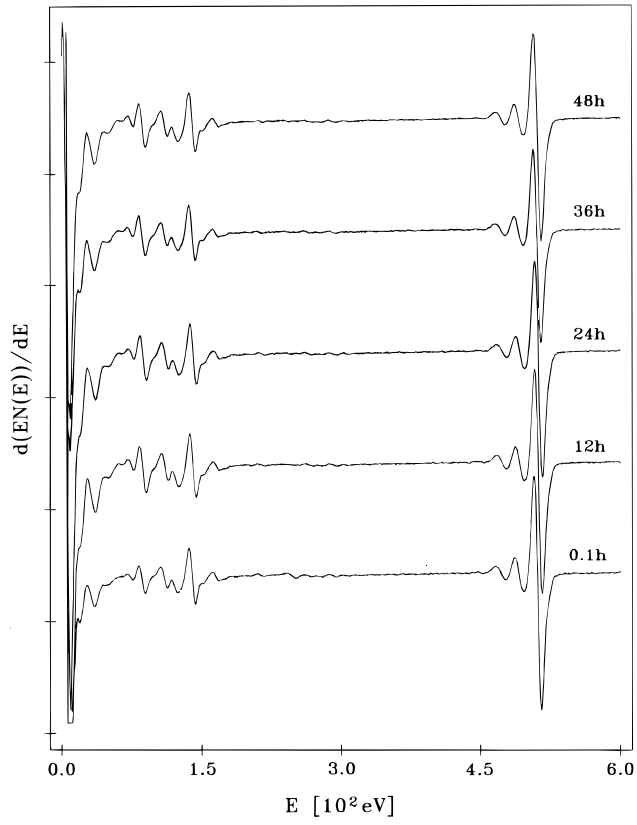

Figure 6. The charge-compensated spectra of YS–ZrO_2 in 5×10^{-8} Torr O_2. Irradiation time is indicated in each spectrum. ($E_P = 2.5$ keV, $\alpha = 0°$.)

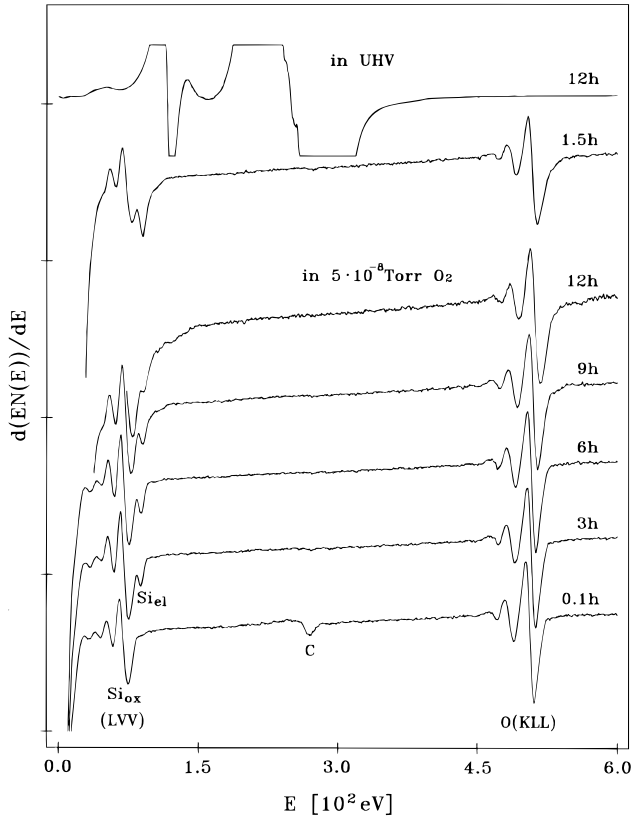

Figure 7. The AES spectra for SiO_2 in an oxygen atmosphere of 5×10^{-8} Torr O_2; for comparison, two spectra without oxygen exposure are displayed at the top. Irradiation time is indicated in each spectrum. ($E_P = 1.5$ keV, $\alpha = 30°$.)

Fig. 5 the charge compensation in 1×10^{-4} Torr Ar and in 5×10^{-8} Torr O_2 is compared for a primary energy of 3 keV and normal incidence; it is obvious that the O_2 environment is much more efficient for the reduction of electron beam-induced effects than the Ar environment, even though the Ar pressure is 5000 times higher.

The charge-compensated spectra of YS–ZrO_2, collected under normal incidence using electrons with an impact energy of 2.5 keV, are shown in Fig. 6. No charging is observed in an appropriate oxygen atmosphere. When applying 1×10^{-4} Torr Ar to the YS–ZrO_2 sample under the same primary parameters, a charge-up of 980 eV builds up after 12 h of exposure; in addition, the carbon contamination on the surface becomes more noticeable than without gas.

The spectra of SiO_2 at the primary energy of 1.5 keV at 5×10^{-8} Torr O_2 are plotted in Fig. 7. For comparison, two spectra measured without additional exposure to oxygen under the same primary parameters are plotted, and the irradiation time is given for each spectrum. In the O_2 environment the sample remains uncharged for at least 12 h of electron irradiation. However, without gas the sample begins to charge after only 1.5 h of irradiation. Interestingly, the carbon peak seen for the lowest exposure time is not seen in the other spectra. Obviously, the residual surface carbon species is removed by the exposure to oxygen, possibly by the formation of carbon oxides, which desorb.

DISCUSSION

Charging processes

On all samples a lateral differential charging in the initial stage of the charge-up process could be observed. This can be understood from the Gaussian profile of the primary electron intensity: the differential charging leads to an inhomogeneous charging potential in the measuring zone, which broadens the Auger peaks and diverts the secondary electrons to larger angles from the primary incidence; consequently, more secondary electrons reach the specimen carousel and cause a rise of the target current (I_T). The split peak (in the differentiated spectra), which shifts to higher energy during the irradiation, is caused by the electrons from the centre of the zone. Simultaneously, the target current, which is dominated by the secondary electrons, increases. The electrons from the edge of the irradiated zone (less strongly charged) produce the peak (in the differentiated spectra), which has only a small shift from the original position of the Auger peak; as soon as the irradiated measuring zone is homogeneously charged, this peak is no longer visible, and the target current remains constant.

The charge potential obtained for a given primary energy and incident angle also depends on the primary current density and the sample history. By sample history we denote all effects caused by previous irradiations; such effects have been observed on irradiated single crystals of quartz, amorphous SiO_2 [7] and pure

ZrO_2.[8] In the present study such effects could be observed also on Al_2O_3 and YS–ZrO_2. In the charging process the sample history induces a stronger charging on the pre-irradiated zone than on the virgin parts of the same sample. This phenomenon is more obvious for SiO_2 and YS–ZrO_2 than for Al_2O_3.

Negative charging is attributed to the presence of defect centres, which offer trap states in the bandgap.[9,10] These defect centres may be created by electron bombardment; for instance, ESD of the oxygen anion can occur on the investigated samples. Additionally, intrinsic defects can be modified by the irradiation, thus creating charge traps. Our results show a correlation between the reduction of charging and oxygen deficiency. This suggests that if the defects, such as oxygen vacancies from ESD, are located at the surface they can be restored in suitable environments like O_2. This is the case for Al_2O_3. Further experiments on polycrystalline Al_2O_3 samples (not presented here) show a very similar behaviour. We therefore conclude that sample structure has little influence on charge trapping. The strong history effects of SiO_2 and YS–ZrO_2 make it likely that, besides the surface defect centres, charge traps located deeper inside the materials may be induced by the electron bombardment.

Charge compensation

Traditional methods. The auxiliary electron beam with an energy of 400 eV enhances the secondary yield δ on Al_2O_3 up to $\delta \sim 4$.[11] This enhances also the ESD of surface anions. Consequently, the surface becomes more deficient in oxygen and a contamination of the surface by residual gas becomes more likely. Both effects modify δ strongly, so that after an irradiation period with both electron beams no difference could be observed in the charge potential with or without the auxiliary electron beam. In this case the auxiliary electron beam cannot be expected to reduce the sample charge-up.

Charge reduction by a positive bias on the irradiated surface can be explained by the field-enhanced secondary emission. A positive bias of 100 V corresponds to a field strength of $<10^6$ V cm^{-1} in the irradiated zone. The breakdown field strength for Al_2O_3 [12] and SiO_2 [13] is in the range of 10^6–10^7 V cm^{-1}; a drastic charge reduction requires a positive bias, offering an electric field equivalent to or even higher than the breakdown field strength of the samples.

The charging phenomena can be reduced by increasing the bulk conductivity or by annealing the induced defects: by heating of the Al_2O_3 and SiO_2 samples to 600 °C, neither of these effects can be achieved, at least not under continuous electron bombardment with higher primary energies. We have found that ESD could be enhanced by specimen heating. This phenomenon can be understood on the basis of oxygen diffusion: the activation energy for migration of an oxygen vacancy amounts to 1.76 eV,[14] and a short-range diffusion is possible with an energy of 0.55 eV.[15] The electron beam produces oxygen vacancies at the surface and the oxygen vacancies can diffuse into the bulk. Thus, the oxygen-deficient layer produced by specimen heating can extend into the materials. Therefore, this method can modify the surface stoichiometry.

An explanation for the charge compensation in the Ar environment has been proposed by Ohlendorf *et al.*:[6] in 1×10^{-4} Torr Ar the charge is reduced by Auger neutralization of the Ar^+ ions ionized by the primary and secondary electrons near the irradiated zone. The charge compensation in an He environment is based on the same mechanism as in Ar, but the ionization cross-section of He is smaller by a factor of ten compared to Ar. Nevertheless, the deep-lying 1s level in He^+ offers a much higher probability for Auger neutralization.[6] This mechanism does also occur with an Ar^+ beam (500 eV). However, we find that it is of minor importance, and reduction of the charging phenomena occurs mainly through sputtering due to its kinetic energy.

Summarizing, one can state that none of these traditional methods for charge-up compensation is able to reduce charging sufficiently or is free from the disturbing effects described above.

Charge reduction in environmental AES with oxygen. We have demonstrated that 5×10^{-8} Torr O_2 has a compensation effect on the irradiation damage and charging phenomena on Al_2O_3 and SiO_2 comparable to an atmosphere of 1×10^{-4} Torr Ar; the effect of this O_2 atmosphere on YS–ZrO_2 is more pronounced than the Ar environment. In order to understand the compensation process, an Ar environment of 5×10^{-8} Torr is used in AES on Al_2O_3; it has been found that 5×10^{-8} Torr Ar hardly reduces the electron beam effects. This result implies that for charge compensation in 1×10^{-4} Torr Ar and 5×10^{-8} Torr O_2, different mechanisms occur. We propose that the first step of the charging is the production of oxygen vacancies on top of the surface by ESD. Subsequently, these vacancies may diffuse into the bulk, producing the bulk charge-up. We therefore suggest that in 5×10^{-8} Torr O_2 the compensation of the charge is due to the immediate reoxidation of the oxygen vacancies on top of the surface. A 5×10^{-8} Torr Ar atmosphere could offer neither a sufficient Ar^+ density nor a sufficient oxygen intrinsic partial pressure for the compensation of the electron beam effects. This model explains the simultaneous reduction of charging, oxygen deficiency and carbon contamination.

Charge compensation in environmental AES using O_2, Ar and He results from the direct reaction of the gaseous molecules or molecular ions with the irradiated surface. A satisfying compensation could be achieved only if the charging is located in the surface layer or stretches slowly into the bulk. This is the case for Al_2O_3. For YS–ZrO_2 and SiO_2 the charges extend deeper into the materials and thus the compensation is less efficient than on Al_2O_3. Nevertheless, we have demonstrated that charge reduction by an O_2 atmosphere is the most efficient for these substances. We expect that this method will work also on other oxide insulators.

Exploratory investigations on non-oxide ceramics such as Si_3N_4 and AlN have shown that even in these cases an oxygen environment of 5×10^{-8} Torr produces a charge reduction up to 20%. This can possibly be understood by the passivation of the surface defects: broken bonds of the surface defects are saturated by oxygen uptake.[16] However, a gaseous environment in

these cases is far less efficient than for the studied oxides.

CONCLUSIONS

Charging of insulating oxides is dependent on the specific resistance, chemical bonding, impurities, intrinsic defects and irradiation resistance. For the same sample and under the same primary parameters the charging process is still dependent on the sample history, particularly any previous irradiation damage. The charging phenomena could not be traced down to one mechanism. However, it seems reasonable to suppose that charging is mainly related to the defects that are induced or modified by the electron bombardment. Such defects, e.g. anion vacancies, act as electron traps.

Several traditional methods used for charge reduction are examined for their efficiency, particularly on single-crystal Al_2O_3. The auxiliary electron gun and biasing with a positive potential at the analysed surface are not efficient methods under long-term electron bombardment; additional disturbing effects, such as the electron elastic peak, the enhancement of ESD when applying the auxiliary gun and the shift of Auger peaks that results when biasing the positive potential, prevent their practical use for AES. Heating up to several hundred degrees centigrade could not achieve a charge compensation on Al_2O_3 nor on SiO_2; it enhances ESD and induces segregation of defects, thus leading to a change of the surface stoichiometry. Environmental AES by applying 1×10^{-4} Torr Ar or He achieves charge compensation on Al_2O_3 and charge reduction on SiO_2, but on YS–ZrO_2 it is less effective and shows harmful effects due to carbon contamination.

The important finding of this work is that an O_2 atmosphere of $<5 \times 10^{-8}$ Torr at the location of the analysed surface provides an efficient compensation of both the irradiation damage and the charge phenomena on all investigated oxides. Under electron irradiation of energy up to 8 keV and for normal incidence, Al_2O_3 is charge-free for days in 5×10^{-8} Torr O_2; charging on SiO_2 and YS–ZrO_2 could be reduced markedly at energies up to 8 keV. In addition, ESD of Al_2O_3 and YS–ZrO_2 is compensated in this way, and for all studied samples no carbon contamination appears. Furthermore, exploratory investigations show comparable results for polycrystalline Al_2O_2, MgO-stabilized ZrO_2, plasma-sprayed $MgAl_2O_4$ and an enamel based on 70% SiO_2.

In addition, the compensation effects of the gaseous environment give insight into the charging process on each substance. In principle one can make a distinction whether the charging occurs on the top of the surface mainly or extends in the material: in the former case the electron beam damage lies mainly on the surface or stretches some depth into the bulk after long irradiation; in the latter case the defects can be induced simultaneously on top and below the surface. As a result, further systematic studies of the interaction of the electron beam with the substances and of the charging mechanism become possible.

So far we have shown that environmental AES with O_2 is suitable for the analysis of clean, stoichiometric oxides. The application of environmental AES with O_2 to non-oxide insulators will be studied in a future paper. Although, we have not performed systematic studies so far, we feel that environmental AES with O_2 will also be applicable to atomic/molecular adsorption, such as chlorine, on metal oxide surfaces. However, eventual reactions between O_2 and the adsorbate species may cause additional problems that have not been well-studied so far. Thus, in such cases AES should be combined with techniques that give information on the electronic structure of the adsorbate-covered surface.

Acknowledgements

Financial support of the Deutsche Forschungsgemeinschaft (SFB 180) is gratefully acknowledged. We thank G. Borchardt (Technische Univesität Clausthal) for providing us with some of the studied samples.

REFERENCES

1. W. Wei, *J. Vac. Sci. Technol.* **A6**(4), 2576 (1988).
2. S. Ichimura, H. E. Bauer, H. Seiler and S. Hofmann, *Surf. Interface Anal.* **14**, 250 (1989).
3. G. Barth, R. Linder and C. Bryson, *Surf. Interface Anal.* **11**, 307 (1988).
4. J. Kirschner, *Scanning Electron Microsc.* **1**, 215 (1976).
5. C. Le Gressus, F. Valin, M. Gautier, J. P. Duraud, J. Cazaux and H. Okuzumi, *Scanning* **12**, 203 (1990).
6. G. Ohlendorf, W. Koch, V. Kempter and G. Borchardt, *Surf. Interface Anal.* **17**, 947 (1991).
7. D. L. Carroll, D. L. Doering and P. Xiong-Skiba, *J. Vac. Sci. Technol.* **A11**, 2312 (1993).
8. K.-O. Axelsson, K.-E. Keck and B. Kasemo, *Appl. Surf. Sci.* **25**, 217 (1986).
9. J. P. Vigouroux, J. P. Duraud, A. Le Moel, C. Le Gressus and D. L. Griscom, *J. Appl. Phys.* **57**, 5139 (1985).
10. M. Marczewski, I. Strzalkowski and J. Baranowski, in *The Physics and Technology of Amorphous SiO_2*, ed. by R. A. B. Devine, p. 119. Plenum Press, New York, (1988).
11. K. Kanaya, S. Ono and F. Ishigaki, *J. Phys. D* **11**, 2425 (1978).
12. S. M. Rowland, R. M. Hill and L. A. Dissado, *J. Phys. C* **19**, 6263 (1986).
13. K. Hamano, *Jpn. J. Appl. Phys.* **13**, 1085 (1974).
14. K. P. R. Reddy and A. R. Cooper, *J. Am. Ceram. Soc.* **65**, 634 (1982).
15. G. P. Pellsand and A. Y. Stathopoulos, *Radiat. Eff.* **74**, 181 (1983).
16. N. Lieske and R. Hezel, *Thin Solid Films* **51**, 217 (1979).